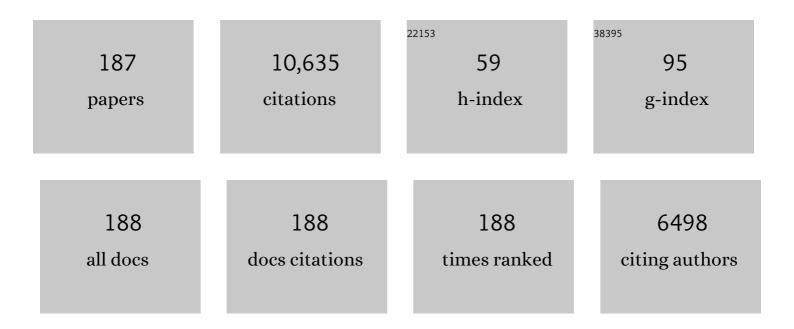
List of Publications by Year in descending order

Source: https://exaly.com/author-pdf/7915588/publications.pdf Version: 2024-02-01



#	Article	IF	CITATIONS
1	Effect of alkali hydroxide on calcium silicate hydrate (C-S-H). Cement and Concrete Research, 2022, 151, 106636.	11.0	57
2	Fast Room-Temperature Mg <sup>2+</sup> Conductivity in Mg(BH <sub>4</sub> ) <sub>2</sub> ·1.6NH <sub>3</sub> –Al <sub>2</sub> O <sub>3</sub> Nanocomposites. Journal of Physical Chemistry Letters, 2022, 13, 2211-2216.	4.6	18
3	Effect of Water–Solid Mixing Sequence and Crystallization Water of Calcium Sulphate on the Hydration of C3A. Materials, 2022, 15, 2297.	2.9	1
4	Impact of sulphate source on the hydration of ternary pastes of Portland cement, calcium aluminate cement and calcium sulphate. Cement and Concrete Composites, 2022, 131, 104502.	10.7	12
5	Characterization of Monochromate and Hemichromate AFm Phases and Chromate-Containing Ettringite by 1H, 27Al, and 53Cr MAS NMR Spectroscopy. Minerals (Basel, Switzerland), 2022, 12, 371.	2.0	1
6	Effect of sulfate on CO2 binding efficiency of recycled alkaline materials. Cement and Concrete Research, 2022, 157, 106804.	11.0	16
7	Methylamine Lithium Borohydride as Electrolyte for Allâ€Solidâ€State Batteries. Angewandte Chemie - International Edition, 2022, 61, .	13.8	20
8	Methylamine Lithium Borohydride as Electrolyte for Allâ€Solidâ€State Batteries. Angewandte Chemie, 2022, 134, .	2.0	2
9	Semi-dry carbonation of recycled concrete paste. Journal of CO2 Utilization, 2022, 63, 102111.	6.8	28
10	<sup>11</sup> B Nuclear Spin–Electron Spin Interactions in <sup>11</sup> B MAS NMR Spectra of Paramagnetic Metal Borohydrides. Journal of Physical Chemistry C, 2021, 125, 1113-1124.	3.1	3
11	Effect of alkalis on enforced carbonation of cement paste: Mechanism of reaction. Journal of the American Ceramic Society, 2021, 104, 1076-1087.	3.8	15
12	Effect of alkalis on products of enforced carbonation of cement paste. Construction and Building Materials, 2021, 291, 123203.	7.2	27
13	Pair distribution function and <sup>71</sup> Ga NMR study of aqueous Ga <sup>3+</sup> complexes. Chemical Science, 2021, 12, 14420-14431.	7.4	6
14	Creep in reactive colloidal gels: A nanomechanical study of cement hydrates. Physical Review Research, 2021, 3, .	3.6	14
15	Incorporation of Sodium and Aluminum in Cementitious Calcium-Alumino-Silicate-Hydrate C-(A)-S-H Phases Studied by <sup>23</sup> Na, <sup>27</sup> Al, and <sup>29</sup> Si MAS NMR Spectroscopy. Journal of Physical Chemistry C, 2021, 125, 27975-27995.	3.1	27
16	Influence of low curing temperatures on the tensile response of low clinker strain hardening UHPFRC under full restraint. Cement and Concrete Research, 2020, 128, 105940.	11.0	12
17	Fe(III) uptake by calcium silicate hydrates. Applied Geochemistry, 2020, 113, 104460.	3.0	31
18	Probing the validity of the spinel inversion model: a combined SPXRD, PDF, EXAFS and NMR study of	3.3	11

#	Article	IF	CITATIONS
19	Impact of Mg substitution on the structure and pozzolanic reactivity of calcium aluminosilicate (CaO-Al2O3-SiO2) glasses. Cement and Concrete Research, 2020, 138, 106231.	11.0	30
20	Shaped Hierarchical H-ZSM-5 Catalysts for the Conversion of Dimethyl Ether to Gasoline. Industrial & amp; Engineering Chemistry Research, 2020, 59, 17689-17707.	3.7	9
21	Ammine Magnesium Borohydride Nanocomposites for All-Solid-State Magnesium Batteries. ACS Applied Energy Materials, 2020, 3, 9264-9270.	5.1	53
22	Ammine Lanthanum and Cerium Borohydrides, <i>M</i> (BH <sub>4</sub> ) <sub>3</sub> · <i>n</i> NH <sub>3</sub> ; Trends in Synthesis, Structures, and Thermal Properties. Inorganic Chemistry, 2020, 59, 7768-7778.	4.0	19
23	Effect of carbonated cement paste on composite cement hydration and performance. Cement and Concrete Research, 2020, 134, 106090.	11.0	111
24	Immobilized piperazine on the surface of graphene oxide as a heterogeneous bifunctional acid–base catalyst for the multicomponent synthesis of 2-amino-3-cyano-4 <i>H</i> -chromenes. Green Chemistry, 2020, 22, 4604-4616.	9.0	32
25	Hydration of polyphase Ca <sub>3</sub> SiO <sub>5</sub> â€Ca <sub>3</sub> Al <sub>2</sub> O <sub>6</sub> in the presence of gypsum and Na <sub>2</sub> SO <sub>4</sub> . Journal of the American Ceramic Society, 2020, 103, 6461-6474.	3.8	8
26	Kinetics of enforced carbonation of cement paste. Cement and Concrete Research, 2020, 131, 106013.	11.0	93
27	CO2 mineralisation of Portland cement: Towards understanding the mechanisms of enforced carbonation. Journal of CO2 Utilization, 2020, 38, 398-415.	6.8	69
28	Phase assemblage and microstructure of cement paste subjected to enforced, wet carbonation. Cement and Concrete Research, 2020, 130, 105990.	11.0	109
29	A hydrophilic heterogeneous cobalt catalyst for fluoride-free Hiyama, Suzuki, Heck and Hirao cross-coupling reactions in water. Green Chemistry, 2020, 22, 1353-1365.	9.0	36
30	Effect of Temperature on the Hydration of White Portland Cement–Metakaolin Blends Studied by 29Si and 27Al MAS NMR. RILEM Bookseries, 2020, , 283-292.	0.4	0
31	Reactivity of supplementary cementitious materials (SCMs) in cement blends. Cement and Concrete Research, 2019, 124, 105799.	11.0	421
32	Dissolution kinetics of calcined kaolinite and montmorillonite in alkaline conditions: Evidence for reactive Al(V) sites. Journal of the American Ceramic Society, 2019, 102, 7720-7734.	3.8	51
33	Nanoscale Ordering and Depolymerization of Calcium Silicate Hydrates in the Presence of Alkalis. Journal of Physical Chemistry C, 2019, 123, 24873-24883.	3.1	30
34	Potassium octahydridotriborate: diverse polymorphism in a potential hydrogen storage material and potassium ion conductor. Dalton Transactions, 2019, 48, 8872-8881.	3.3	34
35	Structure and reactivity of synthetic CaO-Al2O3-SiO2 glasses. Cement and Concrete Research, 2019, 120, 77-91.	11.0	90
36	Optical Sensing of pH and O <sub>2</sub> in the Evaluation of Bioactive Self-Healing Cement. ACS Omega, 2019, 4, 20237-20243.	3.5	16

#	Article	IF	CITATIONS
37	Synthesis of ZSM-23 (MTT) zeolites with different crystal morphology and intergrowths: effects on the catalytic performance in the conversion of methanol to hydrocarbons. Catalysis Science and Technology, 2019, 9, 6782-6792.	4.1	7
38	Sulfate resistance of calcined clay – Limestone – Portland cements. Cement and Concrete Research, 2019, 116, 238-251.	11.0	85
39	Identification of Distinct Framework Aluminum Sites in Zeolite ZSM-23: A Combined Computational and Experimental <sup>27</sup> Al NMR Study. Journal of Physical Chemistry C, 2019, 123, 7831-7844.	3.1	19
40	A quantitative study of the C3A hydration. Cement and Concrete Research, 2019, 115, 145-159.	11.0	74
41	High Zn/Al ratios enhance dehydrogenation vs hydrogen transfer reactions of Zn-ZSM-5 catalytic systems in methanol conversion to aromatics. Journal of Catalysis, 2018, 362, 146-163.	6.2	120
42	Design of a Nanometric AlTi Additive for MgB <sub>2</sub> -Based Reactive Hydride Composites with Superior Kinetic Properties. Journal of Physical Chemistry C, 2018, 122, 7642-7655.	3.1	29
43	The Charge-Balancing Role of Calcium and Alkali Ions in Per-Alkaline Aluminosilicate Glasses. Journal of Physical Chemistry B, 2018, 122, 3184-3195.	2.6	14
44	Hydrate Phase Assemblages in Calcium Sulfoaluminate – Metakaolin – Limestone Blends. RILEM Bookseries, 2018, , 352-357.	0.4	6
45	Synthesis and thermal decomposition of potassium tetraamidoboranealuminate, K[Al(NH2BH3)4]. International Journal of Hydrogen Energy, 2018, 43, 311-321.	7.1	13
46	Efficient Solar-Driven Hydrogen Transfer by Bismuth-Based Photocatalyst with Engineered Basic Sites. Journal of the American Chemical Society, 2018, 140, 16711-16719.	13.7	58
47	Structural Investigation of Ye'elimite, Ca <sub>4</sub> Al <sub>6</sub> O <sub>12</sub> SO <sub>4</sub> , by <sup>27</sup> Al MAS and MQMAS NMR at Different Magnetic Fields. Journal of Physical Chemistry C, 2018, 122, 12077-12089.	3.1	16
48	Distribution of Aluminum over the Tetrahedral Sites in ZSM-5 Zeolites and Their Evolution after Steam Treatment. Journal of Physical Chemistry C, 2018, 122, 15595-15613.	3.1	82
49	Hydrogenation properties of lithium and sodium hydride – <i>closo</i> -borate, [B <sub>10</sub> H <sub>10</sub> ] <sup>2â^'</sup> and [B <sub>12</sub> H <sub>12</sub> ] <sup>2â^'</sup> , composites. Physical Chemistry Chemical Physics, 2018, 20, 16266-16275.	2.8	18
50	Identification of Reactive Sites in Calcined Kaolinite and Montmorillonite from a Combination of Chemical Methods and Solid-State NMR Spectroscopy. RILEM Bookseries, 2018, , 404-408.	0.4	2
51	Friedel's salt profiles from thermogravimetric analysis and thermodynamic modelling of Portland cement-based mortars exposed to sodium chloride solution. Cement and Concrete Composites, 2017, 78, 73-83.	10.7	244
52	Resolution of the Two Aluminum Sites in Ettringite by <sup>27</sup> Al MAS and MQMAS NMR at Very High Magnetic Field (22.3 T). Journal of Physical Chemistry C, 2017, 121, 4011-4017.	3.1	32
53	Role of calcium on chloride binding in hydrated Portland cement–metakaolin–limestone blends. Cement and Concrete Research, 2017, 95, 205-216.	11.0	207
54	Immobilized Lanthanum(III) Triflate on Graphene Oxide as a New Multifunctional Heterogeneous Catalyst for the One-Pot Five-Component Synthesis of Bis(pyrazolyl)methanes. ACS Sustainable Chemistry and Engineering, 2017, 5, 4598-4606.	6.7	17

#	Article	IF	CITATIONS
55	Physical performances of alkaliâ€activated portland cementâ€glassâ€limestone blends. Journal of the American Ceramic Society, 2017, 100, 4159-4172.	3.8	8
56	lonic liquids grafted onto graphene oxide as a new multifunctional heterogeneous catalyst and its application in the one-pot multi-component synthesis of hexahydroquinolines. New Journal of Chemistry, 2017, 41, 6219-6225.	2.8	22
57	Influence of the Ca/Si ratio on the compressive strength of cementitious calcium–silicate–hydrate binders. Journal of Materials Chemistry A, 2017, 5, 17401-17412.	10.3	232
58	Structural characterization of marine nano-quartz in chalk and flint from North Sea Tertiary chalk reservoirs for oil and gas. American Mineralogist, 2017, 102, 1402-1417.	1.9	2
59	Synthesis, Structure, and Li-Ion Conductivity of LiLa(BH <sub>4</sub> ) <sub>3</sub> X, X = Cl, Br, I. Journal of Physical Chemistry C, 2017, 121, 19010-19021.	3.1	32
60	Dynamic Solid-State NMR Experiments Reveal Structural Changes for a Methyl Silicate Nanostructure on Deuterium Substitution. Journal of Physical Chemistry C, 2017, 121, 26507-26518.	3.1	1
61	The structure-directing amine changes everything: structures and optical properties of two-dimensional thiostannates. Acta Crystallographica Section B: Structural Science, Crystal Engineering and Materials, 2017, 73, 931-940.	1.1	8
62	Early stage dissolution characteristics of aluminosilicate glasses with blast furnace slag―and flyâ€ashâ€like compositions. Journal of the American Ceramic Society, 2017, 100, 1941-1955.	3.8	105
63	Thermodynamic modeling of hydrated white Portland cement–metakaolin–limestone blends utilizing hydration kinetics from 29Si MAS NMR spectroscopy. Cement and Concrete Research, 2016, 86, 29-41.	11.0	101
64	One-pot Synthesis of Terminal Vinylphosphonates Catalyzed by Pyridine Grafted GO as Reusable Acid-Base Bifunctional Catalyst. ChemistrySelect, 2016, 1, 2945-2951.	1.5	6
65	NMR and EPR Studies of Free-Radical Intermediates from Experiments Mimicking the Winds on Mars: A Sink for Methane and Other Gases. Journal of Physical Chemistry C, 2016, 120, 26138-26149.	3.1	11
66	Metal borohydride formation from aluminium boride and metal hydrides. Physical Chemistry Chemical Physics, 2016, 18, 27545-27553.	2.8	15
67	Solid state synthesis, structural characterization and ionic conductivity of bimetallic alkali-metal yttrium borohydrides MY(BH <sub>4</sub> ) <sub>4</sub> (M = Li and Na). Journal of Materials Chemistry A, 2016, 4, 8793-8802.	10.3	37
68	Experimental studies and thermodynamic modeling of the carbonation of Portland cement, metakaolin and limestone mortars. Cement and Concrete Research, 2016, 88, 60-72.	11.0	207
69	Properties of magnesium silicate hydrates (M-S-H). Cement and Concrete Research, 2016, 79, 323-332.	11.0	228
70	Pozzolanic reactivity of a calcined interstratified illite/smectite (70/30) clay. Cement and Concrete Research, 2016, 79, 101-111.	11.0	77
71	Quantification of the boron speciation in alkali borosilicate glasses by electron energy loss spectroscopy. Scientific Reports, 2015, 5, 17526.	3.3	17
72	Phase Diagram for the NaBH <sub>4</sub> –KBH <sub>4</sub> System and the Stability of a Na <sub>1–<i>x</i></sub> K <sub><i>x</i></sub> BH <sub>4</sub> Solid Solution. Journal of Physical Chemistry C, 2015, 119, 27919-27929.	3.1	27

JÃ,RGEN SKIBSTED

#	Article	IF	CITATIONS
73	Influence of silica fume on the microstructure of cement pastes: New insights from 1H NMR relaxometry. Cement and Concrete Research, 2015, 74, 116-125.	11.0	150
74	Composition, silicate anion structure and morphology of calcium silicate hydrates (C-S-H) synthesised by silica-lime reaction and by controlled hydration of tricalcium silicate (C <sub>3</sub> S). Advances in Applied Ceramics, 2015, 114, 362-371.	1.1	99
75	Influence of the Ca/Si ratio of the C–S–H phase on the interaction with sulfate ions and its impact on the ettringite crystallization pressure. Cement and Concrete Research, 2015, 69, 37-49.	11.0	148
76	Carbonation of C–S–H and C–A–S–H samples studied by 13 C, 27 Al and 29 Si MAS NMR spectroscopy Cement and Concrete Research, 2015, 71, 56-65.	<sup>'.</sup> 11.0	292
77	TC 238-SCM: hydration and microstructure of concrete with SCMs. Materials and Structures/Materiaux Et Constructions, 2015, 48, 835-862.	3.1	189
78	Trends in Syntheses, Structures, and Properties for Three Series of Ammine Rare-Earth Metal Borohydrides, M(BH <sub>4</sub> ) <sub>3</sub> · <i>n</i> NH <sub>3</sub> (M = Y, Gd, and Dy). Inorganic Chemistry, 2015, 54, 7402-7414.	4.0	41
79	Phase Assemblages in Hydrated Portland Cement, Calcined Clay and Limestone Blends From Solid-State 27Al and 29Si MAS NMR, XRD, and Thermodynamic Modeling. RILEM Bookseries, 2015, , 109-115.	0.4	3
80	Thermodynamic Modeling of Portland Cement—Metakaolin—Limestone Blends. RILEM Bookseries, 2015, , 143-149.	0.4	1
81	Effect of the Partial Replacement of CaH <sub>2</sub> with CaF <sub>2</sub> in the Mixed System CaH <sub>2</sub> + MgB <sub>2</sub> . Journal of Physical Chemistry C, 2014, 118, 28409-28417.	3.1	17
82	Aluminum Incorporation in the C–S–H Phase of White Portland Cement–Metakaolin Blends Studied by <sup>27</sup> <scp><scp>Al</scp> and <sup>29</sup><scp><scp>Si</scp> MAS NMR</scp> Spectroscopy. Journal of the American Ceramic Society, 2014, 97, 2662-2671.</scp>	3.8	119
83	Fluoride ions as structural probe-ions in <sup>19</sup> F MAS NMR studies of cement materials and thermally activated SCMs. Advances in Cement Research, 2014, 26, 233-246.	1.6	2
84	A sink for methane on Mars? The answer is blowing in the wind. Icarus, 2014, 236, 24-27.	2.5	67
85	Synthesis, Crystal Structure, Thermal Decomposition, and <sup>11</sup> B MAS NMR Characterization of Mg(BH <sub>4</sub> ) <sub>2</sub> (NH <sub>3</sub> BH <sub>3</sub> ) <sub>2</sub> . Journal of Physical Chemistry C, 2014, 118, 12141-12153.	3.1	41
86	Magic-angle spinning solid-state multinuclear NMR on low-field instrumentation. Journal of Magnetic Resonance, 2014, 238, 20-25.	2.1	6
87	Hydrogen reversibility of LiBH <sub>4</sub> –MgH <sub>2</sub> –Al composites. Physical Chemistry Chemical Physics, 2014, 16, 8970-8980.	2.8	23
88	Thermal Activation of a Pure Montmorillonite Clay and Its Reactivity in Cementitious Systems. Journal of Physical Chemistry C, 2014, 118, 11464-11477.	3.1	83
89	(NH <sub>4</sub> ) <sub>4</sub> Sn <sub>2</sub> S <sub>6</sub> ·3H <sub>2</sub> O: Crystal Structure, Thermal Decomposition, and Precursor for Textured Thin Film. Chemistry of Materials, 2014, 26, 4494-4504.	6.7	19
90	Nanoconfined NaAlH <sub>4</sub> : prolific effects from increased surface area and pore volume. Nanoscale, 2014, 6, 599-607.	5.6	47

#	Article	IF	CITATIONS
91	2LiBH4–MgH2–0.13TiCl4 confined in nanoporous structure of carbon aerogel scaffold for reversible hydrogen storage. Journal of Alloys and Compounds, 2014, 599, 78-86.	5.5	36
92	Hydrogen Storage Capacity Loss in a LiBH <sub>4</sub> –Al Composite. Journal of Physical Chemistry C, 2013, 117, 7423-7432.	3.1	45
93	Hydrogen–fluorine exchange in NaBH4–NaBF4. Physical Chemistry Chemical Physics, 2013, 15, 18185.	2.8	52
94	13C chemical shift anisotropies for carbonate ions in cement minerals and the use of 13C, 27Al and 29Si MAS NMR in studies of Portland cement including limestone additions. Cement and Concrete Research, 2013, 52, 100-111.	11.0	59
95	The Effect of Alkali Ions on the Incorporation of Aluminum in the Calcium Silicate Hydrate ( <scp><scp>C</scp>&lt; scp&gt;â€"<scp>S</scp>a€"<scp>S</scp>a€"<scp>A</scp>masses and the second former th</scp>	3.8	118
96	Investigations of the thermal decomposition of MBH4–2NH3BH3, M=Na, K. Journal of Alloys and Compounds, 2013, 580, S287-S291.	5.5	18
97	Clay reactivity: Production of alkali activated cements. Applied Clay Science, 2013, 73, 11-16.	5.2	87
98	Hydrogen Sorption in the LiH–LiF–MgB <sub>2</sub> System. Journal of Physical Chemistry C, 2013, 117, 17360-17366.	3.1	9
99	Improved hydrogen storage kinetics of nanoconfined LiBH <sub>4</sub> -MgH <sub>2</sub> reactive hydride composites catalyzed with nickel Nanoparticles. Materials Research Society Symposia Proceedings, 2012, 1441, 1.	0.1	5
100	Role of internal coke for deactivation of ZSM-5 catalysts after low temperature removal of coke with NO2. Catalysis Science and Technology, 2012, 2, 1196.	4.1	30
101	2LiBH <sub>4</sub> –MgH <sub>2</sub> in a Resorcinol–Furfural Carbon Aerogel Scaffold for Reversible Hydrogen Storage. Journal of Physical Chemistry C, 2012, 116, 1526-1534.	3.1	44
102	Alkaline solution/binder ratio as a determining factor in the alkaline activation of aluminosilicates. Cement and Concrete Research, 2012, 42, 1242-1251.	11.0	139
103	LiCe(BH <sub>4</sub> ) <sub>3</sub> Cl, a New Lithium-Ion Conductor and Hydrogen Storage Material with Isolated Tetranuclear Anionic Clusters. Chemistry of Materials, 2012, 24, 1654-1663.	6.7	128
104	Hydration of Blended <scp>P</scp> ortland Cements Containing Calciumâ€Aluminosilicate Glass Powder and Limestone. Journal of the American Ceramic Society, 2012, 95, 403-409.	3.8	23
105	Characterization of the Network Structure of Alkali-Activated Aluminosilicate Binders by Single- and Double-Resonance 29si {27al} Mas Nmr Experiments. , 2012, , 707-715.		0
106	Synthesis of <sup>17</sup> O-Labeled Cs <sub>2</sub> WO <sub>4</sub> and Its Ambient- and Low-Temperature Solid-State <sup>17</sup> O MAS NMR Spectra. Inorganic Chemistry, 2011, 50, 7676-7684.	4.0	10
107	Improved Hydrogen Storage Kinetics of Nanoconfined NaAlH <sub>4</sub> Catalyzed with TiCl <sub>3</sub> Nanoparticles. ACS Nano, 2011, 5, 4056-4064.	14.6	110
108	Structural studies of lithium zinc borohydride by neutron powder diffraction, Raman and NMR spectroscopy. Journal of Alloys and Compounds, 2011, 509, S698-S704.	5.5	40

#	Article	IF	CITATIONS
109	Mixedâ€Anion and Mixed ation Borohydride KZn(BH <sub>4</sub> )Cl <sub>2</sub> : Synthesis, Structure and Thermal Decomposition. European Journal of Inorganic Chemistry, 2010, 2010, 1608-1612.	2.0	48
110	Characterisation of cement hydrate phases by TEM, NMR and Raman spectroscopy. Advances in Cement Research, 2010, 22, 233-248.	1.6	141
111	Incorporation of Phosphorus Guest Ions in the Calcium Silicate Phases of Portland Cement from <sup>31</sup> P MAS NMR Spectroscopy. Inorganic Chemistry, 2010, 49, 5522-5529.	4.0	20
112	Thermal Polymorphism and Decomposition of Y(BH <sub>4</sub> ) <sub>3</sub> . Inorganic Chemistry, 2010, 49, 3801-3809.	4.0	96
113	Evidence of Intermediate-Range Order Heterogeneity in Calcium Aluminosilicate Glasses. Chemistry of Materials, 2010, 22, 4471-4483.	6.7	69
114	Structure and Characterization of KSc(BH <sub>4</sub> ) <sub>4</sub> . Journal of Physical Chemistry C, 2010, 114, 19540-19549.	3.1	95
115	Improved evidence for the existence of an intermediate phase during hydration of tricalcium silicate. Cement and Concrete Research, 2010, 40, 875-884.	11.0	100
116	Solid-state 51V MAS NMR spectroscopy determines component concentration and crystal phase in co-crystallised mixtures of vanadium complexes. CrystEngComm, 2010, 12, 2826.	2.6	11
117	A Series of Mixedâ€Metal Borohydrides. Angewandte Chemie - International Edition, 2009, 48, 6659-6663.	13.8	228
118	Improved quantification of alite and belite in anhydrous Portland cements by 29Si MAS NMR: Effects of paramagnetic ions. Solid State Nuclear Magnetic Resonance, 2009, 36, 32-44.	2.3	73
119	Site Preferences of Fluoride Guest Ions in the Calcium Silicate Phases of Portland Cement from 29Si{19F} CP-REDOR NMR Spectroscopy. Journal of the American Chemical Society, 2009, 131, 14170-14171.	13.7	30
120	Structure and Dynamics of Hydrous Surface Species on Aluminaâ^'Boria Catalysts and Their Precursors from <sup>1</sup> H, <sup>2</sup> H, <sup>11</sup> B, and <sup>27</sup> Al MAS NMR Spectroscopy. Journal of Physical Chemistry C, 2009, 113, 2475-2486.	3.1	11
121	Site Preferences of NH4+in Its Solid Solutions with Cs2WS4and Rb2WS4from Multinuclear Solid-State MAS NMR. Inorganic Chemistry, 2009, 48, 1787-1789.	4.0	11
122	New opportunities in acquisition and analysis of natural abundance complex solid-state 33S MAS NMR spectra: (CH3NH3)2WS4. Physical Chemistry Chemical Physics, 2009, 11, 6981.	2.8	19
123	Microstructure engineering of Portland cement pastes and mortars through addition of ultrafine layer silicates. Cement and Concrete Composites, 2008, 30, 686-699.	10.7	68
124	Sensitivity enhancement in natural-abundance solid-state 33S MAS NMR spectroscopy employing adiabatic inversion pulses to the satellite transitions. Journal of Magnetic Resonance, 2008, 190, 316-326.	2.1	39
125	Characterization of cement minerals, cements and their reaction products at the atomic and nano scale. Cement and Concrete Research, 2008, 38, 205-225.	11.0	108
126	Structural Environments for Boron and Aluminum in Aluminaâ^'Boria Catalysts and Their Precursors from <sup>11</sup> B and <sup>27</sup> Al Single- and Double-Resonance MAS NMR Experiments. Journal of Physical Chemistry C, 2008, 112, 7210-7222.	3.1	26

#	Article	IF	CITATIONS
127	Single-Crystal Growth and Characterization of Disilver(I) Monofluorophosphate(V), Ag2PO3F:  Crystal Structure, Thermal Behavior, Vibrational Spectroscopy, and Solid-State 19F, 31P, and 109Ag MAS NMR Spectroscopy. Inorganic Chemistry, 2007, 46, 801-808.	4.0	28
128	Evaluation of27Al and51V Electric Field Gradients and the Crystal Structure for Aluminum Orthovanadate (AlVO4) by Density Functional Theory Calculations. Journal of Physical Chemistry B, 2006, 110, 5975-5983.	2.6	34
129	Probing Crystal Structures and Transformation Reactions of Ammonium Molybdates by14N MAS NMR Spectroscopy. Inorganic Chemistry, 2006, 45, 10873-10881.	4.0	24
130	A new aluminium-hydrate species in hydrated Portland cements characterized by 27Al and 29Si MAS NMR spectroscopy. Cement and Concrete Research, 2006, 36, 3-17.	11.0	285
131	Effects of T2-relaxation in MAS NMR spectra of the satellite transitions for quadrupolar nuclei: a 27Al MAS and single-crystal NMR study of alum KAl(SO4)2·12H2O. Journal of Magnetic Resonance, 2005, 173, 209-217.	2.1	5
132	Structure refinement of CsNO3(II) by coupling of 14N MAS NMR experiments with WIEN2k DFT calculations. Chemical Physics Letters, 2005, 402, 133-137.	2.6	40
133	Formation and Structure of Conjugated Salen-Cross-Linked Polymers and Their Application in Asymmetric Heterogeneous Catalysis. European Journal of Organic Chemistry, 2005, 2005, 342-347.	2.4	34
134	Refinement of Borate Structures from 11B MAS NMR Spectroscopy and Density Functional Theory Calculations of 11B Electric Field Gradients. Journal of Physical Chemistry A, 2005, 109, 1989-1997.	2.5	68
135	A solid-state 14N magic-angle spinning NMR study of some amino acids. Journal of Magnetic Resonance, 2004, 166, 262-272.	2.1	70
136	Characterization of white Portland cement hydration and the C-S-H structure in the presence of sodium aluminate by 27Al and 29Si MAS NMR spectroscopy. Cement and Concrete Research, 2004, 34, 857-868.	11.0	291
137	The Complete 51V MAS NMR Spectrum of Surface Vanadia Nanoparticles on Anatase (TiO2):  Vanadia Surface Structure of a DeNOx Catalyst. Journal of the American Chemical Society, 2004, 126, 4926-4933.	13.7	51
138	11B Chemical Shift Anisotropies in Borates from 11B MAS, MQMAS, and Single-Crystal NMR Spectroscopy. Journal of Physical Chemistry A, 2004, 108, 586-594.	2.5	73
139	Solid state NMR studies of the hydration of molecular sieve AIPO-36. Studies in Surface Science and Catalysis, 2004, 154, 1238-1245.	1.5	1
140	Determination of nitrogen chemical shift anisotropy from the second-order cross-term in 14N MAS NMR spectroscopy. Chemical Physics Letters, 2003, 377, 426-432.	2.6	19
141	29Si cross-polarization magic-angle spinning NMR spectroscopy––an efficient tool for quantification of thaumasite in cement-based materials. Cement and Concrete Composites, 2003, 25, 823-829.	10.7	14
142	Small 51V chemical shift anisotropy for LaVO4 from MQMAS and MAS NMR spectroscopy. Solid State Nuclear Magnetic Resonance, 2003, 23, 107-115.	2.3	12
143	Unusual observation of nitrogen chemical shift anisotropies in tetraalkylammonium halides by 14N MAS NMR spectroscopy. Solid State Nuclear Magnetic Resonance, 2003, 24, 218-235.	2.3	27
144	Hydration of Portland cement in the presence of clay minerals studied by <sup>29</sup> Si and <sup>27</sup> Al MAS NMR spectroscopy. Advances in Cement Research, 2003, 15, 103-112.	1.6	38

#	Article	IF	CITATIONS
145	Incorporation of Aluminum in the Calcium Silicate Hydrate (Câ^'Sâ^'H) of Hydrated Portland Cements:Â A High-Field27Al and29Si MAS NMR Investigation. Inorganic Chemistry, 2003, 42, 2280-2287.	4.0	321
146	A thermodynamic model for predicting the stability of thaumasite. Cement and Concrete Composites, 2003, 25, 867-872.	10.7	28
147	29Si Chemical Shift Anisotropies in Calcium Silicates from High-Field29Si MAS NMR Spectroscopy. Inorganic Chemistry, 2003, 42, 2368-2377.	4.0	81
148	14N MAS NMR Spectroscopy and Quadrupole Coupling Data in Characterization of the IV ↔ III Phase Transition in Ammonium Nitrate. Journal of Physical Chemistry B, 2002, 106, 3026-3032.	2.6	37
149	Characterization of the αâ <sup>~</sup> β Phase Transition in Friedels Salt (Ca2Al(OH)6Cl·2H2O) by Variable-Temperature 27Al MAS NMR Spectroscopy. Journal of Physical Chemistry A, 2002, 106, 6676-6682.	2.5	29
150	Hydrothermal Synthesis, Single-Crystal Structure Analysis, and Solid-State NMR Characterization of Zn2(OH)0.14(3)F0.86(3)(PO4). Journal of Solid State Chemistry, 2002, 164, 42-50.	2.9	9
151	β-VO2—a V(IV) or a mixed-valence V(III)–V(V) oxide—studied by 51V MAS NMR spectroscopy. Chemical Physics Letters, 2002, 356, 73-78.	2.6	17
152	Aluminum Orthovanadate (AlVO4):Â Synthesis and Characterization by27Al and51V MAS and MQMAS NMR Spectroscopy. Inorganic Chemistry, 2002, 41, 6432-6439.	4.0	42
153	Crystal structure of α-Mg2V2O7 from synchrotron X-ray powder diffraction and characterization by 51V MAS NMR spectroscopy. Dalton Transactions RSC, 2001, , 3214-3218.	2.3	24
154	Resolving multiple 27Al sites in AlVO4 by 27Al MAS NMR spectroscopy at 21.15 Tesla. Chemical Communications, 2001, , 2690-2691.	4.1	6
155	14N MAS NMR Spectroscopy:Â The Nitrate Ion. Journal of the American Chemical Society, 2001, 123, 5098-5099.	13.7	68
156	Solid-State NMR Characterization of the Mineral Searlesite and Its Detection in Complex Synthesis Mixtures. Inorganic Chemistry, 2001, 40, 5906-5912.	4.0	13
157	51V MAS NMR Investigation of51V Quadrupole Coupling and Chemical Shift Anisotropy in Divalent Metal Pyrovanadates. Journal of Physical Chemistry B, 2001, 105, 420-429.	2.6	66
158	59Co Chemical Shift Anisotropy and Quadrupole Coupling for K3Co(CN)6 from MQMAS and MAS NMR Spectroscopy. Solid State Nuclear Magnetic Resonance, 2001, 20, 23-34.	2.3	15
159	Phosphorus-doped thin silica films characterized by magic-angle spinning nuclear magnetic resonance spectroscopy. Journal of Applied Physics, 2001, 89, 4134-4138.	2.5	0
160	Influence of cement constitution and temperature on chloride binding in cement paste. Advances in Cement Research, 2000, 12, 57-64.	1.6	24
161	Zeolites by confined space synthesis – characterization of the acid sites in nanosized ZSM-5 by ammonia desorption and 27Al/29Si-MAS NMR spectroscopy. Microporous and Mesoporous Materials, 2000, 39, 393-401.	4.4	158
162	Synthesis and characterization of basic bismuth(III) nitrates. Dalton Transactions RSC, 2000, , 265-270.	2.3	69

#	Article	IF	CITATIONS
163	Characterization of Divalent Metal Metavanadates by51V Magic-Angle Spinning NMR Spectroscopy of the Central and Satellite Transitions. Inorganic Chemistry, 2000, 39, 2135-2145.	4.0	57
164	Solid-State QCPMG NMR of Low-γ Quadrupolar Metal Nuclei in Natural Abundance. Journal of the American Chemical Society, 2000, 122, 7080-7086.	13.7	123
165	Characterization of a New Hexasodium Diphosphopentamolybdate Hydrate, Na6[P2Mo5O23]·7H2O, by 23Na MQMAS NMR Spectroscopy and X-ray Powder Diffraction. Inorganic Chemistry, 2000, 39, 4130-4136.	4.0	8
166	Solid-state NMR of RbVO3. A comparison of experiments for retrieving chemical shielding and quadrupole coupling tensorial interactions. Solid State Nuclear Magnetic Resonance, 1999, 14, 203-210.	2.3	6
167	35Cl and37Cl Magic-Angle Spinning NMR Spectroscopy in the Characterization of Inorganic Perchlorates. Inorganic Chemistry, 1999, 38, 1806-1813.	4.0	47
168	Characterization of Na5P3O10 Polymorphs by 23Na MAS, 23Na MQMAS, and 31P MAS NMR Spectroscopy. Inorganic Chemistry, 1999, 38, 84-92.	4.0	30
169	Characterization of Mo(CO)6by95Mo Single-Crystal NMR Spectroscopy. Journal of Physical Chemistry A, 1999, 103, 9144-9149.	2.5	25
170	Variable-Temperature 87Rb Magic-Angle Spinning NMR Spectroscopy of Inorganic Rubidium Salts. Journal of Physical Chemistry A, 1999, 103, 7958-7971.	2.5	35
171	Quantitative Aspects of 27Al MAS NMR of Calcium Aluminoferrites. Advanced Cement Based Materials, 1998, 7, 57-59.	0.3	33
172	51V Chemical Shielding and Quadrupole Coupling in Ortho- and Metavanadates from51V MAS NMR Spectroscopy. Inorganic Chemistry, 1998, 37, 3083-3092.	4.0	76
173	Discussion: Quantification of thaumasite in cementitious materials by29Si{1H} cross-polarization magic-angle NMR spectroscopy. Advances in Cement Research, 1997, 9, 135-138.	1.6	3
174	Pulsed field gradient multiple-quantum MAS NMR spectroscopy of half-integer spin quadrupolar nuclei. Chemical Physics Letters, 1997, 281, 44-48.	2.6	24
175	133Cs Chemical Shielding Anisotropies and Quadrupole Couplings from Magic-Angle Spinning NMR of Cesium Saltsâ€. The Journal of Physical Chemistry, 1996, 100, 14872-14881.	2.9	62
176	Quadrupole Coupling and Anisotropic Shielding from Single-Crystal NMR of the Central Transition for Quadrupolar Nuclei.87Rb NMR of RbClO4and Rb2SO4. Journal of Magnetic Resonance Series A, 1996, 122, 111-119.	1.6	58
177	Quantification of thaumasite in cementitious materials by <sup>29</sup> Si { <sub>1</sub> H} cross-polarization magic-angle spinning NMR spectroscopy. Advances in Cement Research, 1995, 7, 69-83.	1.6	29
178	Line shapes and widths of MAS sidebands for 27Al satellite transitions. Multinuclear MAS NMR of tugtupite Na8Al2Be2Si8O24Cl2. Solid State Nuclear Magnetic Resonance, 1995, 5, 239-255.	2.3	23
179	Quantification of calcium silicate phases in Portland cements by 29Si MAS NMR spectroscopy. Journal of the Chemical Society, Faraday Transactions, 1995, 91, 4423.	1.7	68
180	23Na Magic-angle spinning nuclear magnetic resonance of central and satellite transitions in the characterization of the anhydrous, dihydrate, and mixed phases of sodium molybdate and tungstate. Solid State Nuclear Magnetic Resonance, 1994, 3, 29-38.	2.3	17

#	Article	IF	CITATIONS
181	Direct observation of aluminium guest ions in the silicate phases of cement minerals by 27 Al MAS NMR spectroscopy. Journal of the Chemical Society, Faraday Transactions, 1994, 90, 2095.	1.7	81
182	51V MAS NMR spectroscopy: determination of quadrupole and anisotropic shielding tensors, including the relative orientation of their principal-axis systems. Chemical Physics Letters, 1992, 188, 405-412.	2.6	155
183	Satellite transitions in MAS NMR spectra of quadrupolar nuclei. Journal of Magnetic Resonance, 1991, 95, 88-117.	0.5	83
184	High-speed spinning versus high magnetic field in MAS NMR of quadrupolar nuclei. 27Al MAS NMR of 3CaOA·Al2O3. Journal of Magnetic Resonance, 1991, 92, 669-676.	0.5	16
185	Correlation between 29Si NMR chemical shifts and mean Siî—,O bond lengths for calcium silicates. Chemical Physics Letters, 1990, 172, 279-283.	2.6	47
186	Magic-angle spinning NMR spectra of satellite transitions for quadrupolar nuclei in solids. Journal of Magnetic Resonance, 1989, 85, 173-180.	0.5	55
187	29Si MAS NMR studies of portland cement components and effects of microsilica on the hydration reaction. Cement and Concrete Research, 1988, 18, 789-798.	11.0	129